Supporting Information

Enhancing the alkaline hydrogen evolution reaction activity through the Ni-Mn_3O_4 nanocomposites

Xu Li,[a] *Peng Fei Liu,*[a] *Le Zhang,*[a] *Meng Yang Zu,*[a] *Yun Xia Yang*[a] *and Hua Gui Yang**,[a]

[a] Key Laboratory for Ultrafine Materials of Ministry of Education, School of Materials Science and Engineering, East China University of Science and Technology, 130 Meilong Road, Shanghai 200237, China.

Experimental Section

Materials: Nickel chloride hexahydrate ($NiCl_2·6H_2O$), manganese (II) chloride tetrahydrate ($MnCl_2·4H_2O$), hydrazine hydrate ($N_2H_4·H_2O$), chlorhydric acid (HCl), and potassium hydroxide (KOH) were obtained from Sinopharm Chemistry Reagent Co., Ltd. Nafion (5wt.%) was obtained from Sigma-Aldrich. All chemicals were used as received without further purication and all aqueous solutions were prepared with ultrapure water (>18.25 MΩ cm) obtained from Millipore system.

Synthesis of Ni-Mn_3O_4/NF nanocomposites: Ni-Mn_3O_4/NF (synthesis of the optimal ratio of Ni:Mn=4:1 is given as an example) nanocomposites were synthesized through a hydrothermal process. $NiCl_2·6H_2O$ (0.29 g, 1.2 mmol) and $MnCl_2·4H_2O$ (0.059 g, 0.3 mmol) were dissolved and mixed in the beaker with 25 ml ultrapure water. 5mL $N_2H_4·H_2O$ (80 wt%) was added to the mixed solution under stirring. The Ni foam (1.6-mm thick, 110 p.p.i., geometric area of 1 cm^2) was cleaned by ultrasonication in 6 M HCl for 5 min to remove the surface oxide layer, washed sequentially by water and acetone. After being dried at 50 ℃ for 10 min, the nickel foam was transferred to a 50 ml Teflon lined stainless steel autoclave with precursor solution for hydrothermal reaction at 180℃ for 24 h. After the autoclave was cooled to room temperature, the Ni-Mn_3O_4/NF was washed with ultrapure water three times and sonicated for 5 min and then dried at 70℃ for 8 h in vacuum oven. The products with different molar ratio of the Ni and Mn were obtained by adjusting the molar ratios of the $NiCl_2 • 6H_2O$ and $MnCl_2 • 4H_2O$ (1:1, 2:1, 3:1, 4:1, 5:1, 1:4) in the precursor solution.

Synthesis of Ni/NF nanocomposites: The synthetic procedure was similar to the above except the absence of $MnCl_2·4H_2O$ in the precursor solution.

Synthesis of Mn_3O_4/NF nanocomposites: The synthetic procedure was similar to the above except the absence of $NiCl_2·6H_2O$ in the precursor solution.

Electrochemical measurements: All the electrochemical tests were performed in a conventional three-electrode system at an electrochemical station (CHI 660E), using Ag/AgCl (3.5 M KCl solution) electrode as the reference electrode, Pt mesh as the counter electrode respectively. The Ni-Mn_3O_4/NF, Ni/NF and Mn_3O_4/NF electrodes were directly used as the working electrode for electrochemical characterizations. All potentials were referenced to reversible hydrogen electrode (RHE) by the following calculations: $E_{RHE} = E_{Ag/AgCl} + 0.059 \times pH + 0.205$. All LSV polarization curves were corrected with 100% iR-compensation. AC impedance measurements were carried out in the same configuration when the working electrode was biased at the η of 200 mV from 10^5 Hz to 0.1 Hz with an AC amplitude of 5 mV. Chronopotentiometric measurement (j = 20 mA cm^{-2}) was performed to evaluate the long-term stability. The electrochemical active surface area (ECSA) was determined by measuring the capacitive current associated with double-layer charging from the scan-rate dependence of cyclic voltammograms (CVs). The potential window of CVs was 0.12 V to 0.22 V *vs*. RHE. The double layer capacitance (C_{dl}) was estimated by plotting the $j = (j_a - j_c)$ at 0.17 V *vs*. RHE against the scan rate. The liner slope is twice of the double layer capacitance C_{dl}.

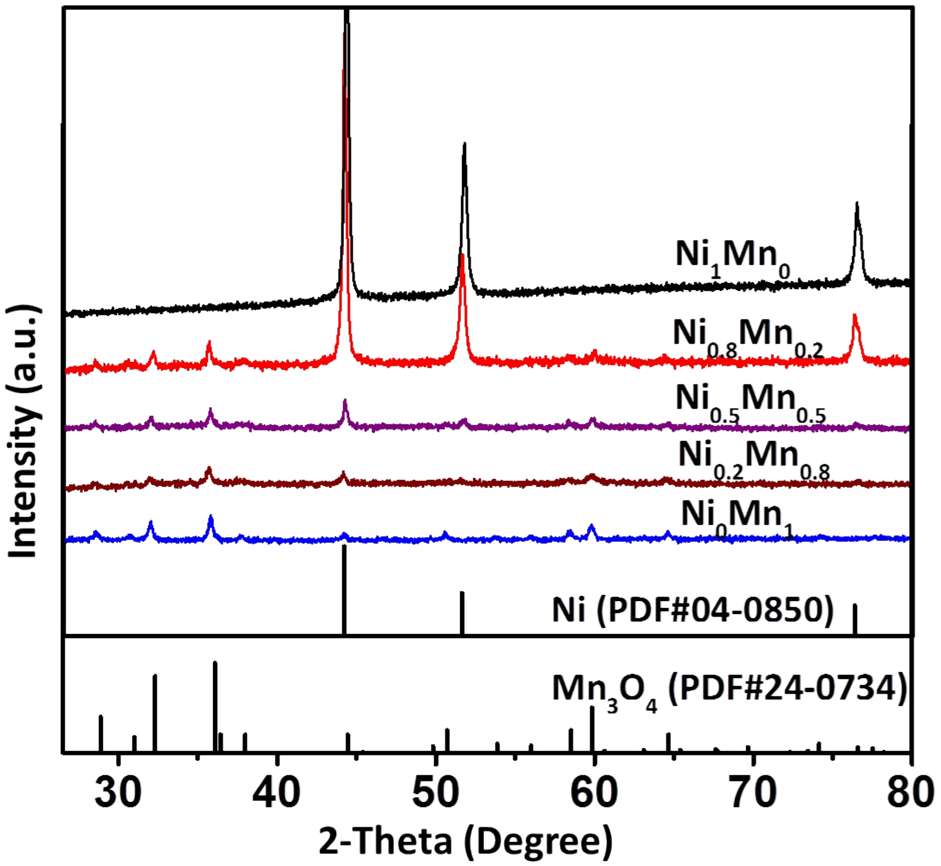

Figure S1. XRD spectra of catalysts obtained in this work with different Ni/Mn atomic ratio.

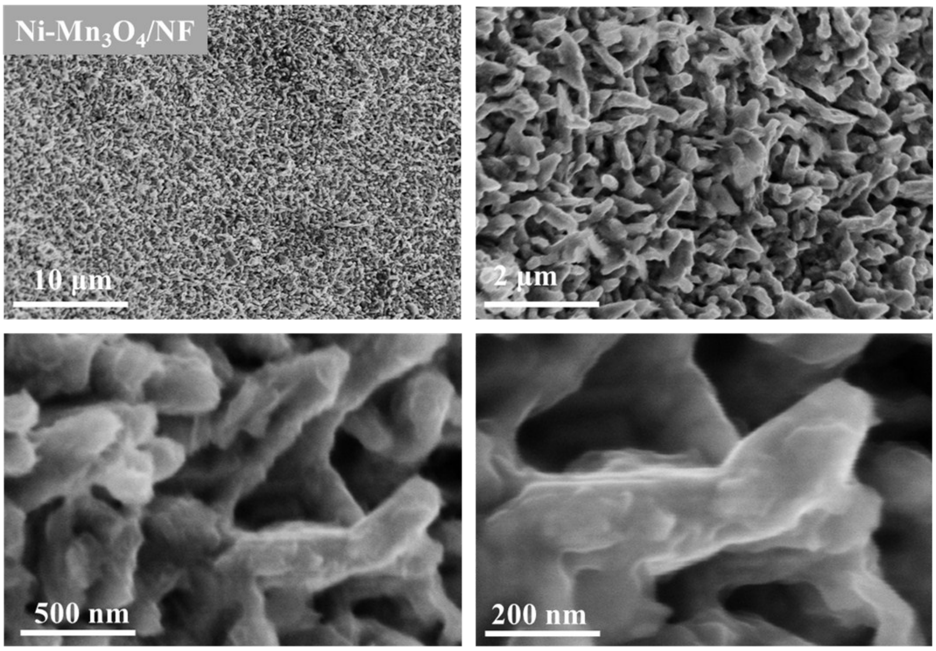

Figure S2. The SEM images of a) Ni-Mn$_3$O$_4$/NF, b) Ni/NF and c) Mn$_3$O$_4$/NF.

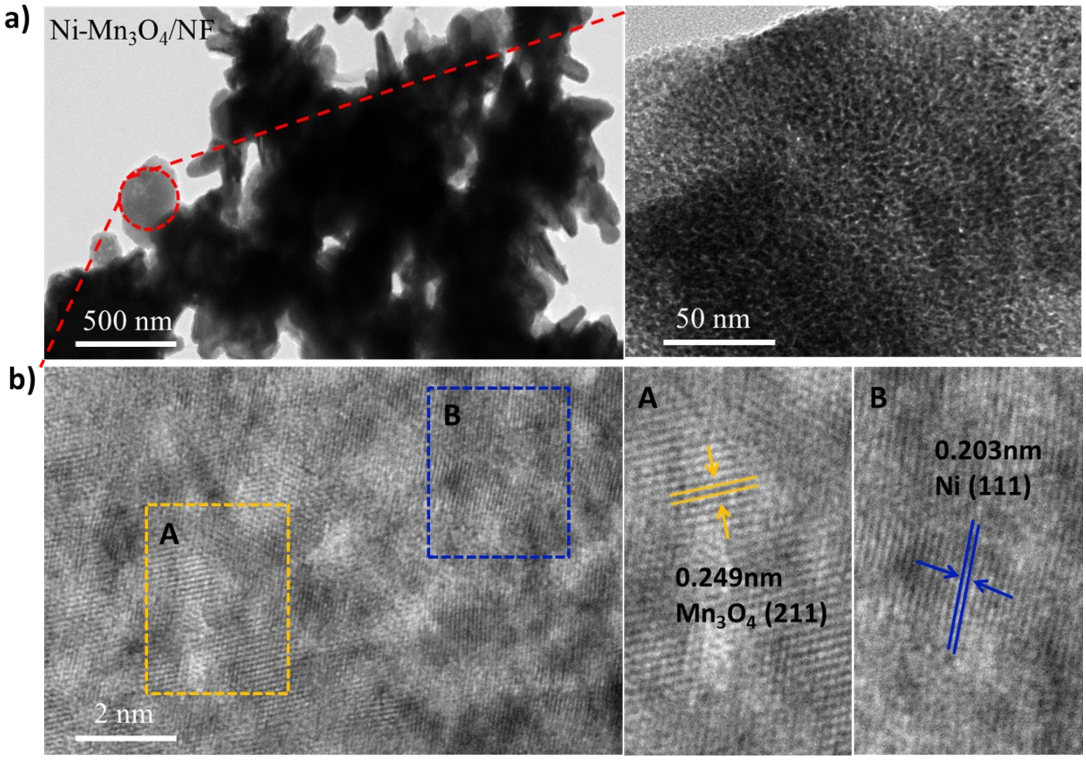

Figure S3. a) TEM and b) HRTEM images of Ni-Mn_3O_4 nanocomposites.

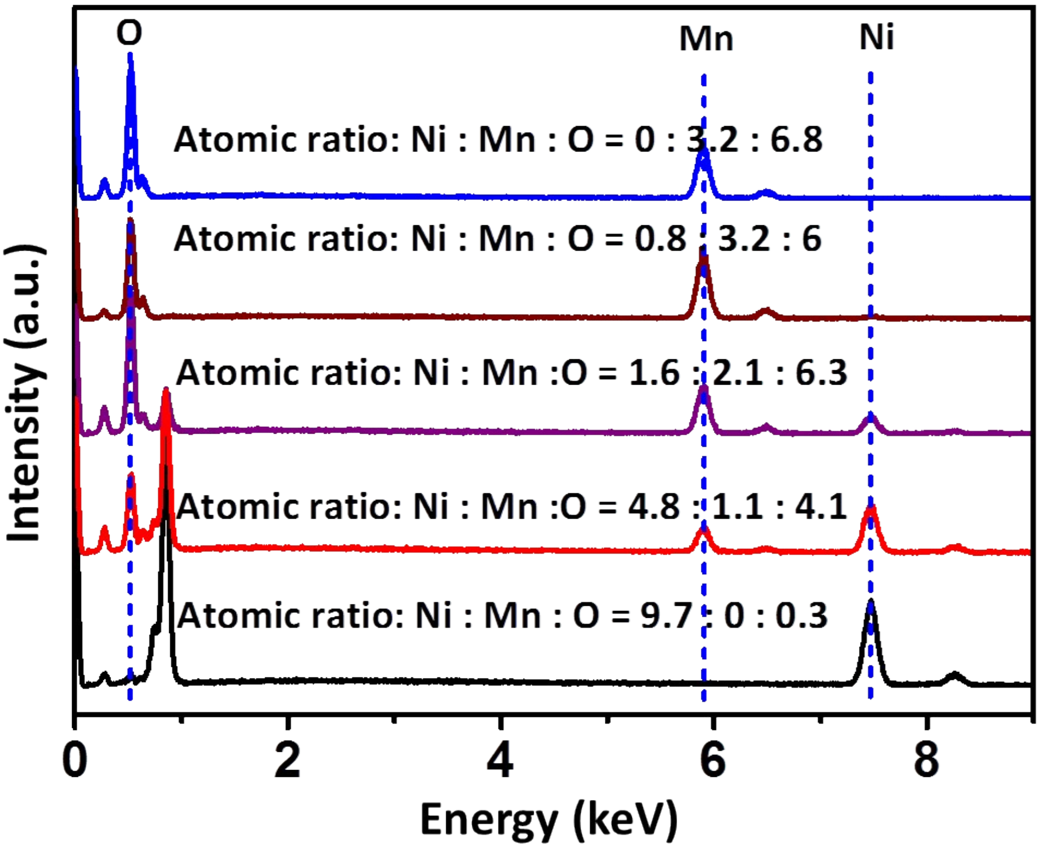

Figure S4. EDX spectra of Ni-Mn_3O_4/NF nanocomposites, revealing different atomic ratios of Ni : Mn.

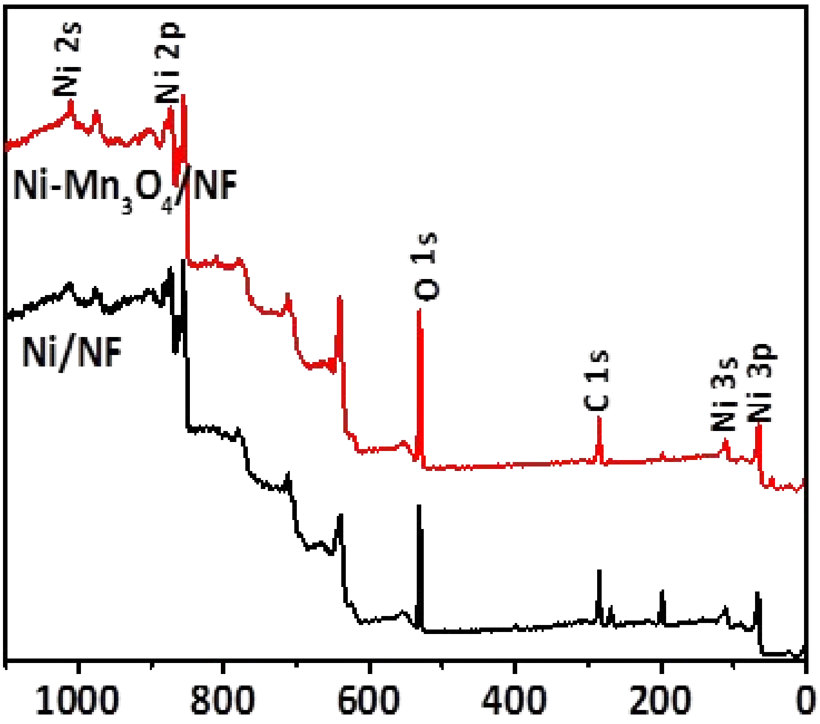

Figure S5. The XPS survey spectra for the Ni-Mn_3O_4/NF and Ni/NF samples.

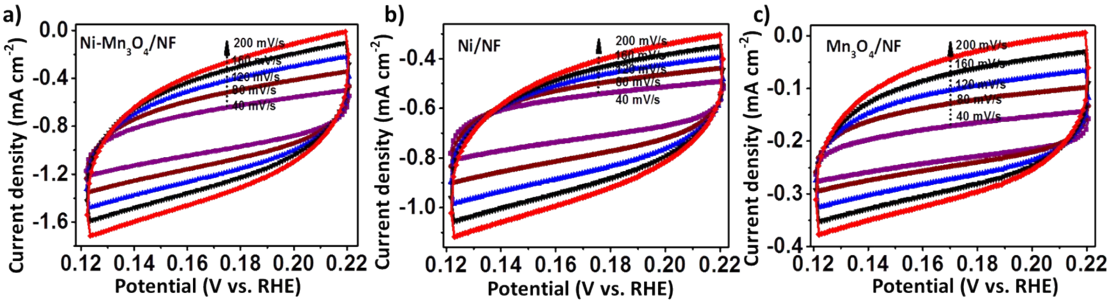

Figure S6. CVs at different scan rates in a potential window where no Faradaic processes occur (0.12 V ~ 0.22 V *vs*. RHE) for (a) Ni-Mn_3O_4/NF, (b) Ni/NF and (c) Mn_3O_4/NF respectively.

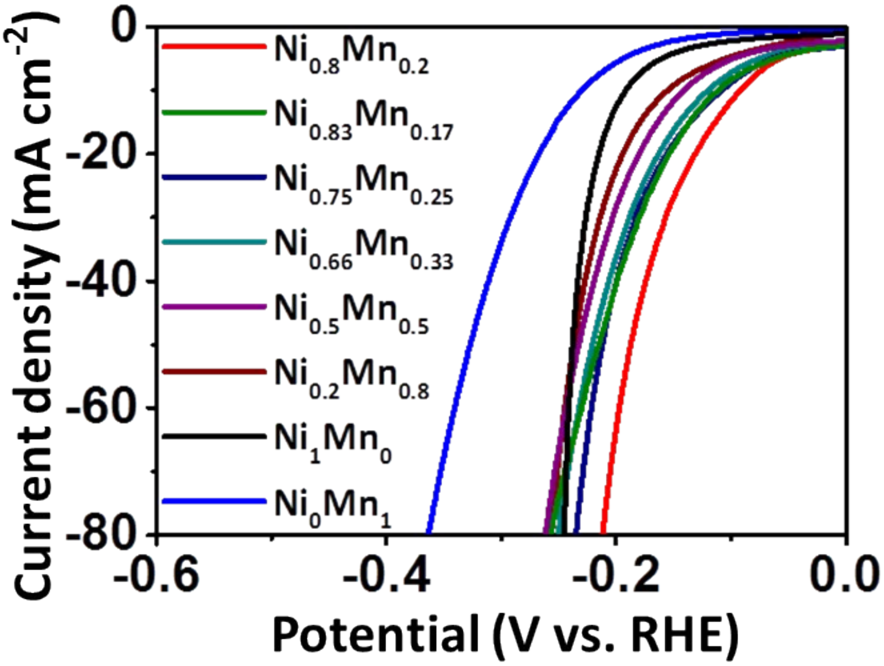

Figure S7. HER polarization curves for all Ni-Mn_3O_4/NF samples in 1 M KOH.